Eur. Phys. J. C (2019) 79:865
https://doi.org/10.1140/epjc/s10052-019-7395-y

THE EUROPEAN PHYSICAL JOURNAL C

Regular Article - Theoretical Physics

Large N_c scaling of meson masses and decay constants

P. Hernández[1], **C. Pena**[2], **F. Romero-López**[1,a]

[1] IFIC (CSIC-UVEG), Edificio Institutos Investigación, Apt. 22085, 46071 Valencia, Spain
[2] Departamento de Física Teórica and Instituto de Física Teórica UAM-CSIC, Universidad Autónoma de Madrid, 28049 Madrid, Spain

Received: 13 August 2019 / Accepted: 11 October 2019 / Published online: 22 October 2019

Abstract We perform an ab initio calculation of the N_c scaling of the low-energy couplings of the chiral Lagrangian of low-energy strong interactions, extracted from the mass dependence of meson masses and decay constants. We compute these observables on the lattice with four degenerate fermions, $N_f = 4$, and varying number of colours, $N_c = 3$–6, at a lattice spacing of $a \simeq 0.075$ fm. We find good agreement with the expected N_c scaling and measure the coefficients of the leading and subleading terms in the large N_c expansion. From the subleading N_c corrections, we can also infer the N_f dependence, that we use to extract the value of the low-energy couplings for different values of N_f. We find agreement with previous determinations at $N_c = 3$ and $N_f = 2, 3$ and also, our results support a strong paramagnetic suppression of the chiral condensate in moving from $N_f = 2$ to $N_f = 3$.

1 Introduction

The 't Hooft limit of QCD [1] is well known to capture correctly most of its non-perturbative features, such as confinement and chiral symmetry breaking. Large N_c inspired approximations are often employed in phenomenological approaches to hadron physics [2–11], but systematic errors from subleading N_c corrections are only naively estimated.

Lattice Field Theory offers the possibility of ab initio explorations of the large N_c limit of QCD, by simulating at different values of N_c [12,13]. Several studies have already been performed. In Ref. [13] a thorough study of mesonic two-point functions was carried out in the quenched approximation, a limit that captures correctly the leading order terms in N_c, but modifies subleading corrections in an uncontrolled way. Furthermore, in Ref. [14] a similar study was performed for $N_c = 2$–5 using $N_f = 2$ dynamical fermions at rather high pion masses.

In addition to the standard approach, the study of QCD in the large N_c limit can also be achieved using reduced models (see [15] for a review). In this context, there has been significant progress regarding the properties of mesons [16–20].

Besides, lattice simulations have been used to perform studies of various observables in theories with different number of colours, flavours or fermion representations in the context of Beyond-the-Standard-Model theories. Some recent results can be found in [21–26] and for recent reviews see [27,28].

In this work, we use previously generated lattice configurations with $N_c = 3$–6 and four dynamical fermions. Our particular choice of N_f has also advantages for weak matrix elements [29]. On these ensembles, we compute meson masses and decay constants as a function of the quark mass at the different values of N_c. We fit these to chiral perturbation theory (ChPT) in order to extract the leading order and next-to-leading order low-energy chiral couplings (LECs). We then study their N_c scaling and extract the first two terms in the 't Hooft series. Our study builds on previous lattice determinations of the LECs for $N_c = 3$ [30–44], whose main results are summarized in [45].

Interestingly, within the large N_c expansion, the $1/N_c$ corrections have a well-defined linear dependence on N_f, while the 't Hooft limit is independent on N_f. Using this fact, we can predict the low-energy couplings at different values of N_f up to higher orders in N_c. This allows us to compare with previous determinations, and check the prediction of *paramagnetic* suppression at large N_f of Refs. [46,47].

This paper is organized as follows. First, we describe chiral perturbation theory predictions and the relation to the large N_c limit in Sect. 2. In Sect. 3, we present the lattice setup that involves a mixed-action formulation. Next, we explain our scale setting procedure at different N_c consistent with 't Hooft scaling in Sect. 4. In Sect. 5 we present the results of our chiral fits to the meson mass and decay constant, first at fixed N_c and then combined with the large N_c expansion.

[a] e-mail: fernando.romero@uv.es

We also present results for theories with different values of N_f, compare with previous literature and discuss systematic uncertainties. We conclude in Sect. 6.

2 Chiral perturbation Theory predictions

The light spectrum of QCD is the result of the pattern of spontaneous chiral symmetry breaking, $SU(N_f)_L \times SU(N_f)_R \to SU(N_f)_{L+R}$. ChPT represents accurately the dynamics of the expected pseudo-Nambu-Goldstone bosons (pNGB), i.e., the lightest non-singlet multiplet of pseudoscalar mesons (the octet for $N_f = 3$), at sufficiently small quark masses. The increase in the number of colours while keeping the 't Hooft coupling constant, $\lambda = g^2 N_c$, is not expected to modify these features. On the other hand, in the large N_c limit, QCD reduces to a theory of narrow and non-interacting resonances and, as a result, the interactions of pNGB within the effective theory decrease with N_c, improving the convergence of the perturbative series. One complication of the large N_c expansion is the role of the singlet pseudoscalar meson, i.e., the η'. Its mass originates in the explicit $U(1)_A$ breaking by the anomaly. In QCD this contribution to the mass is at the cutoff scale of the chiral effective theory and it is therefore integrated out. However, the anomalous contribution to the singlet mass decreases with N_c and in the large N_c limit the η' becomes degenerate with the remaining pNGBs. The effective theory should consequently include an additional singlet pseudoscalar meson in the spectrum. The corresponding effective theory has been studied long ago [48–53]. A new power-counting is needed which involves a simultaneous expansion in $1/N_c$ and the usual chiral expansion in the quark mass and momenta. A consistent power counting was implemented in Refs. [52,53]:

$$\mathcal{O}(\delta) \sim \mathcal{O}(p^2) \sim \mathcal{O}(m_q) \sim \mathcal{O}(m_\pi^2) \sim \mathcal{O}(N_c^{-1}). \tag{1}$$

In the following we will concentrate on the non-singlet multiplet masses and decay constants. We now compare the usual $SU(N_f)$ ChPT to the $U(N_f)$ ChPT for these observables.

2.1 $SU(N_f)$ effective theory

At Leading Order (LO) in the standard $SU(N_f)$ chiral expansion there are only two couplings for any number of degenerate flavours, related to the chiral condensate and the meson decay constant. At Next-to-Leading Order (NLO), and for an arbitrary number of degenerate flavours ($N_f > 3$), 13 more LECs are needed, but only two combinations enter in the observables of interest. For N_f degenerate flavours, ChPT predicts at NLO [54–56]:

$$F_\pi = F\left[1 - \frac{N_f}{2}\frac{M_\pi^2}{(4\pi F_\pi)^2}\log\frac{M_\pi^2}{\mu^2} + 4\frac{M_\pi^2}{F_\pi^2}\left(L_5^r + N_f L_4^r\right)\right], \tag{2}$$

and

$$M_\pi^2 = 2Bm\left[1 + \frac{1}{N_f}\frac{M_\pi^2}{(4\pi F_\pi)^2}\log\frac{M_\pi^2}{\mu^2} + 8\frac{M_\pi^2}{F_\pi^2}\left(2L_8^r - L_5^r + N_f(2L_6^r - L_4^r)\right)\right], \tag{3}$$

in terms of the LO couplings, B, F, and the NLO Gasser–Leutwyler coefficients, $L_{4,5,6,8}^r(\mu)$, defined at the renormalization scale μ.

Equations (2–3) are valid for an arbitrary number of colours, but the LECs scale with N_c as (for a review see [57]):

$$O(N_c) : F^2, L_5, L_8;\ O(1) : B, L_4, L_6. \tag{4}$$

Loop corrections are suppressed in $1/F_\pi^2 = O(1/N_c)$, and hence the loop expansion is expected to converge better at larger N_c.

Keeping only leading and subleading dependence on N_c a convenient parametrization is

$$F = \sqrt{N_c}\left(F_0 + \frac{F_1}{N_c}\right), \qquad B = B_0 + \frac{B_1}{N_c}, \tag{5}$$

and

$$L_5 + N_f L_4 \equiv L_F = N_c L_F^{(0)} + L_F^{(1)}, \tag{6}$$

$$2L_8 - L_5 + N_f(2L_6 - L_4) \equiv L_M = N_c L_M^{(0)} + L_M^{(1)}. \tag{7}$$

Note that according to the scaling of Eq. (4) and the definition of Eq. (7):

$$L_F^{(0)} = \frac{L_5}{N_c} + \mathcal{O}\left(\frac{1}{N_c}\right),$$
$$L_M^{(0)} = \frac{2L_8 - L_5}{N_c} + \mathcal{O}\left(\frac{1}{N_c}\right). \tag{8}$$

The NNLO Lagrangian of the $SU(N_f)$ theory is also known [54–56]. At this order we will instead only use the $U(N_f)$, to which we now turn.

2.2 $U(N_f)$ effective theory

In the $U(N_f)$ ChPT at NLO, i.e., $\mathcal{O}(\delta^1)$, the result can be read from Eqs. (2) and (3) and the different N_c scalings of the LECs in Eqs. (5) and (7):

$$F_\pi = \sqrt{N_c}\left(F_0 + \frac{F_1}{N_c}\right)\left[1 + 4\frac{M_\pi^2}{F_\pi^2}N_c L_F^{(0)} + \mathcal{O}(\delta^2)\right], \tag{9}$$

and

$$M_\pi^2 = 2\left(B_0 + \frac{B_1}{N_c}\right) m \left[1 + 8\frac{M_\pi^2}{F_\pi^2} N_c L_M^{(0)} + \mathcal{O}(\delta^2)\right]. \tag{10}$$

The NLO corrections are not enough to explain the data in this case, therefore going to NNLO is essential. At NNLO new features appear, because the singlet contributes to the mass loop corrections. The necessary results can be found in Ref. [58]. For degenerate flavours, they simplify to:

$$F_\pi = \sqrt{N_c}\left(F_0 + \frac{F_1}{N_c} + \frac{F_2}{N_c^2}\right)\left[1 - \frac{N_f}{2}\frac{M_\pi^2}{(4\pi F_\pi)^2}\log\frac{M_\pi^2}{\mu^2} + 4\frac{M_\pi^2}{F_\pi^2}\left(N_c L_F^{(0)} + L_F^{(1)}\right) + N_c^2 K_F^{(0)}\left(\frac{M_\pi^2}{F_\pi^2}\right)^2 + \mathcal{O}(\delta^3)\right], \tag{11}$$

and

$$M_\pi^2 = 2m\left(B_0 + \frac{B_1}{N_c} + \frac{B_2}{N_c^2}\right) \times \left[1 + \frac{1}{N_f}\frac{M_\pi^2}{(4\pi F_\pi)^2}\log\frac{M_\pi^2}{\mu^2} - \frac{1}{N_f}\frac{M_{\eta'}^2}{(4\pi F_\pi)^2}\log\frac{M_{\eta'}^2}{\mu^2} + 8\frac{M_\pi^2}{F_\pi^2}\left(N_c L_M^{(0)} + L_M^{(1)}\right) + N_c^2 K_M^{(0)}\left(\frac{M_\pi^2}{F_\pi^2}\right)^2 + \mathcal{O}(\delta^3)\right], \tag{12}$$

where $K_{F,M}^{(0)}$ are combinations of $L_F^{(0)}$, $L_M^{(0)}$ and new LECs that appear in the $U(N_f)$ case. For details see [58]. Note that for degenerate quarks, there is no η-η' mixing.

The η' mass in this expression can be taken in the large N_c limit, where it is given by the Witten–Veneziano formula:

$$M_{\eta'}^2 = M_\pi^2 + \frac{2N_f}{F^2}\chi_t \equiv M_\pi^2 + M_0^2, \tag{13}$$

where χ_t is the topological susceptibility in pure Yang–Mills, recently computed in the large N_c limit in Ref. [59].

Note that even though we use the same notation for the LECs in both chiral expansions, they are different: in the $SU(N_f)$ ChPT the LECs encode the effects of integrating out the η'. The matching of the two theories starts at NNLO [53,60] and only affects the coupling B and $L_M^{(1)}$ of the above [53,60]:

$$\begin{aligned}[B]_{SU(N_f)} &= [B]_{U(N_f)}\left(1 - \frac{1}{N_f}\frac{M_0^2}{(4\pi F_\pi)^2}\lambda_0\right), \\ \left[L_M^{(1)}\right]_{SU(N_f)} &= \left[L_M^{(1)}\right]_{U(N_f)} - \frac{1}{8N_f(4\pi)^2}(\lambda_0 + 1),\end{aligned} \tag{14}$$

with $\lambda_0 = \log\frac{M_0^2}{\mu^2}$.

2.3 N_f versus N_c dependence

A diagrammatic analysis of fermion bilinear two point functions shows that within the large N_c expansion, the leading order $N_c \to \infty$ limit is N_f independent and the NLO is $\mathcal{O}(N_f/N_c)$. We should confirm this expectation also in ChPT formulae above, in particular given the explicit dependence on N_f. It turns out that within the $U(N_f)$ expansion, the large N_c expansion yields the expected behaviour: the terms in $1/N_f$ exactly cancel when the large N_c expansion is taken at fixed M_π. We expect therefore that the LECs should also satisfy this same scaling.

On the other hand within the $SU(N_f)$ expansion or in the $U(N_f)$ when $M_\pi \ll M_{\eta'}$, that is when the chiral limit is taken first, anomalous $1/N_f$ terms appear coming from an expansion in $M_\pi/M_{\eta'}$. In the $U(N_f)$ expansion such dependence is explicit, but in the $SU(N_f)$ it permeates to the LECs which can no longer be assumed to have the expected $\mathcal{O}(N_f/N_c)$ dependence, as can be explicitly seen in the matching of $L_M^{(1)}$ in Eq. (14).

This way, at the order we are working, we can assume the expected scaling in N_f of the $U(N_f)$ and $SU(N_f)$ couplings except in the case of $[L_M^{(1)}]_{SU(N_f)}$.

3 Lattice setup

We have generated ensembles for $SU(N_c)$ gauge theory with $N_f = 4$ degenerate dynamical fermions, varying $N_c =$ 3-6, using the HiRep code [61]. Some of them have been already presented in Ref. [62]. We have chosen the Iwasaki gauge action (following previous experience with 2+1+1 simulations [63,64]) and $O(a)$-improved[1] Wilson fermions for the sea quarks. Our simulations use the standard Hybrid Montecarlo (HMC) algorithm with Hasenbusch acceleration. We include five layers in each of the fermionic monomials. Interestingly, we observe that the tuning of the integrator at $N_c = 3$ yields similar results at other values of N_c (at similar pion mass) for the acceptance rate, which we keep at 80–90%. The computational cost of each step in Montecarlo time scales as $\sim N_c^2$, with the advantage of a more efficient parallelization at large N_c.

In order to achieve automatic $O(a)$ improvement and avoid the need of a non-perturbative determination of normalization factors, we employ maximally twisted valence

[1] For $N_c = 3$, we take the perturbative value of $c_{sw} = 1 + c_{sw}^{(1)} g^2$ from Ref. [65], where we use the plaquette-boosted coupling $g^2 = 2N_c/(\beta P) = O(1/N_c)$. For other values of N_c, we use the fact that the one loop coefficient is dominated by the tadpole contribution, which is of order N_c (see Eq. 58 in Ref. [65]). This way, c_{sw} is constant up to subleading corrections in N_c, which have an effect of $O(a^2/N_c)$ in physical observables. The full result cannot be easily reconstructed from Ref. [65].

quarks, i.e., the mixed-action setup [66] previously used in Refs. [67–69]. Maximal twist is ensured by tuning the untwisted bare valence mass, $m^{\rm v}$ to the critical value for which the valence PCAC mass is zero:

$$\lim_{m^{\rm v}\to m_{\rm cr}} m^{\rm v}_{\rm pcac} \equiv \lim_{m^{\rm v}\to m_{\rm cr}} \frac{\partial_0 \langle A^0(x) P(y)\rangle}{2\langle P(x)P(y)\rangle} = 0, \tag{15}$$

where $A^\mu(x) \equiv \bar\Psi(x)\gamma^\mu\gamma^5\Psi(x)$ and $P(x) = \bar\Psi(x)\gamma^5\Psi(x)$. The bare twisted mass parameter μ_0 is tuned such that the pion mass in the sea and valence sectors coincide, $M^{\rm v}_\pi = M^s_\pi$. The normalized meson decay constant F_π can then be obtained from the bare combination [70]:

$$F_\pi = \frac{2\mu_0 \langle 0|P|\pi\rangle_{\rm bare}}{M^2_\pi}. \tag{16}$$

The results for the meson masses and decay constant in the mixed-action setup can be seen in Table 3. We have achieved a good tuning of $m_{\rm pcac}$ and the pseudoscalar masses are compatible within one or two sigma with their pure Wilson value (see Table 1). When the tuning to maximal twist is not perfect, we correct the bare quark mass (and thus F_π) as follows (see also [70]):

$$a\mu_0 \to a\mu_0 \sqrt{1+\left(\frac{Z_A a m_{\rm pcac}}{a\mu_0}\right)^2}, \tag{17}$$

$$aF_\pi \to aF_\pi \sqrt{1+\left(\frac{Z_A a m_{\rm pcac}}{a\mu_0}\right)^2}. \tag{18}$$

where the axial normalization constant, Z_A, can be obtained non-perturbatively by matching the valence bare twisted mass with the PCAC mass measured in the sea sector:

$$\mu_0 = Z_A m^s_{\rm pcac}, \text{ for } M^{\rm v}_\pi = M^s_\pi. \tag{19}$$

4 Scale setting at large N_c

The scale setting for different values of N_c is performed using the gradient flow scale $\sqrt{8t_0}$, via the determination of t_0/a^2. In QCD, with $N_c = 3$, the standard definition of t_0 is:

$$\langle t^2 E(t)\rangle\Big|_{t=t_0} = c = 0.3. \tag{20}$$

The leading dependence in N_c is known [71] in perturbation theory:

$$\langle t^2 E(t)\rangle = \frac{3}{128\pi^2}\frac{N_c^2-1}{N_c}\lambda_{\rm GF}(q), \tag{21}$$

where $\lambda_{\rm GF}(q)$ is the gradient flow 't Hooft coupling at the scale $q = 1/\sqrt{8t}$. Hence, as in Ref. [59], we will generalize t_0 to an arbitrary N_c as:

$$\langle t^2 E(t)\rangle\Big|_{t=t_0} = c(N_c) = \frac{3}{8}\frac{N_c^2-1}{N_c}c(3). \tag{22}$$

Notice that the choice here is not unique. In particular, one could choose another coupling in a different scheme (such as $\overline{\rm MS}$), and this would induce corrections at order $O(N_f/N_c)$ in dimensionful quantities.

We also need the value of t_0 in physical units. This is known from lattice simulations for $N_f = 2$ [72,73] and $N_f = 3$ [74] degenerate quarks and at a reference pion mass $M_{\rm ref} = 420$ MeV:

$$\begin{aligned}\sqrt{t_0}\Big|^{N_f=2}_{M_{\rm ref}} &= 0.1470(14)\ \text{fm},\\ \sqrt{t_0}\Big|^{N_f=3}_{M_{\rm ref}} &= 0.1460(19)\ \text{fm}\end{aligned} \tag{23}$$

We can use these to perform a linear extrapolation to $N_f = 4$, motivated by the weak N_f dependence:

$$\sqrt{t_0}\Big|^{N_f=4}_{M_{\rm ref}} = 0.1450(39)\ \text{fm}. \tag{24}$$

Our scale setting condition involves therefore the dimensionless quantity

$$(M_\pi\sqrt{t_0})\Big|_{M_{\rm ref}} = 0.3091(83). \tag{25}$$

In order to reduce discretization errors we have performed a tree level improvement of t_0. In Ref. [75], lattice perturbation theory is used to improve $\langle t^2E(t)\rangle$ and thus, t_0. The prescription is:

$$\langle t^2E(t)\rangle_a = \langle t^2E(t)\rangle_{\rm imp}\left[1+\sum_n C_{2n}\left(\frac{a^2}{t}\right)^n\right], \tag{26}$$

where the coefficients C_{2n} depend on the gauge action, the flow action and the definition of $E(t)$ (clover or plaquette). The coefficients for the Iwasaki gauge action, the plaquette action for the flow and the clover definition of $E(t)$ are:

$$\begin{aligned}C_2 &= -0.262333,\ C_4 = 0.0936935,\\ C_6 &= -0.048002,\ C_8 = 0.0320211.\end{aligned} \tag{27}$$

The numerical results after the improvement, $t_0^{\rm imp}/a^2$, are shown in Table 1.

Finally, Eq. (25) requires t_0 at $M_{\rm ref}$. The mass dependence of t_0 has been studied in chiral perturbation theory in Ref. [77]. For degenerate flavours it is given by

$$t_0 = t_0^\chi\left(1+k\ M^2\right) + \mathcal{O}(M^4), \tag{28}$$

where $k \propto 1/(F_\pi)^2 = O(1/N_c)$ and so the chiral dependence is suppressed in N_c. We have performed accordingly a linear fit in M^2 to extract the reference value. The mass dependence of $t_0^{\rm imp}$ for the different values of N_c can be seen in Fig. 1. As expected, the slope is suppressed with N_c. The

Table 1 Summary of our ensembles: β, sea quark bare mass parameter, m^s, and sea pion mass M_π^s . We keep $c_{sw} = 1.69$ throughout

Ensemble	$L^3 \times T$	β	am^s	aM_π^s	t_0^{imp}/a^2
3A10	$20^3 \times 36$	1.778	−0.4040	0.2204 (21)	3.263 (50)
3A20	$24^3 \times 48$		−0.4060	0.1845 (14)	3.491 (32)
3A30	$24^3 \times 48$		−0.4070	0.1613 (16)	3.740 (39)
3A40	$32^3 \times 60$		−0.4080	0.1429 (12)	3.855 (27)
4A10	$20^3 \times 36$	3.570	−0.3725	0.2035 (14)	3.494 (45)
4A20	$24^3 \times 48$		−0.3752	0.1805 (7)	3.565 (26)
4A30	$24^3 \times 48$		−0.3760	0.1714 (8)	3.593 (29)
4A40	$32^3 \times 60$		−0.3780	0.1397 (8)	3.723 (23)
5A10	$20^3 \times 36$	5.969	−0.3458	0.2128 (9)	3.532 (17)
5A20	$24^3 \times 48$		−0.3490	0.1802 (6)	3.614 (18)
5A30	$24^3 \times 48$		−0.3500	0.1712 (6)	3.664 (24)
5A40	$32^3 \times 60$		−0.3530	0.1331 (7)	3.776 (19)
6A10	$20^3 \times 36$	8.974	−0.3260	0.2150 (7)	3.619 (17)
6A20	$24^3 \times 48$		−0.3300	0.1801 (5)	3.696 (17)
6A30	$24^3 \times 48$		−0.3311	0.1689 (7)	3.721 (15)
6A40	$32^3 \times 60$		−0.3340	0.1351 (6)	3.820 (17)

Table 2 Results for the $t_0/a^2\big|_{M_{\text{ref}}}$ and the lattice spacing as a function of N_c. The first error is statistical, the second comes from the uncertainty in t_0 in physical units, the third stems from the difference in the definitions of $E(t)$ after improvement, and the fourth are finite volume effects estimated from Ref. [76]

N_c	$t_0/a^2\big\|_{M_{\text{ref}}}$	a ($\times 10^{-2}$ fm)
3	$3.71(4)(7)_{t_0}(12)_a(3)_L$	$7.53(4)(19)_{t_0}(12)_a(3)_L$
4	$3.64(1)(3)_{t_0}(12)_a(3)_L$	$7.60(1)(20)_{t_0}(12)_a(3)_L$
5	$3.69(2)(3)_{t_0}(12)_a(3)_L$	$7.54(2)(20)_{t_0}(12)_a(3)_L$
6	$3.76(1)(2)_{t_0}(12)_a(3)_L$	$7.48(1)(20)_{t_0}(12)_a(3)_L$

results of the scale setting can be seen in Table 2, where we also include the systematic uncertainties. The leading uncertainty comes from the error on the value of t_0 in physical units, the discretization error is estimated from the difference in two definitions of $E(t)$ after improvement, and the finite volume systematic error is estimated from Ref. [76]. As it can be seen, the scale setting yields a uniform lattice spacing for all the values of N_c. From now on, we will quote our results in terms of the lattice spacing $a = 0.0754$ fm, corresponding to $N_c = 5$.

5 Chiral perturbation theory fits

The results for M_π and F_π in the mixed-action setup are presented in Table 3. We want to compare these results to the expectations in ChPT described in Sec. 2 in order to the extract the LECs and study their N_c scaling.

Before addressing the fits, we need to explain some technical issues regarding the finite volume effects, the renormalization scale and the fitting strategy. We then perform fits at a fixed value of N_c to test the ansätze for the N_c scaling of the LECs in Eqs. 5 and 7. After that, we perform simultaneous chiral and N_c fits. We present a selection of relevant results for the latter, and conclude the section with a discussion on systematic errors.

5.1 Finite volume effects

Our ensembles have $M_\pi L > 3.8$ in all cases so we expect finite volume effects to be small and suppressed as $1/N_c$. Still, we find that for the decay constant they can be of $O(1\%)$ and thus we correct them as [78,79]:

$$M_\pi(L) = M_\pi \left[1 + \frac{1}{2N_f}\xi\ \bar{g}_1(M_\pi L) + O(\xi^2)\right], \tag{29}$$

$$F_\pi(L) = F_\pi \left[1 - \frac{N_f}{2}\xi\ \bar{g}_1(M_\pi L) + O(\xi^2)\right], \tag{30}$$

with $\xi \equiv \frac{M_\pi^2}{(4\pi F_\pi)^2}$, while $\bar{g}_1(x)$ is given by

$$\bar{g}_1(x) \xrightarrow{x\gg 1} \frac{24}{x} K_1(x) \sim \frac{24\sqrt{2}}{\sqrt{\pi}} \frac{e^{-x}}{x^{3/2}}. \tag{31}$$

We will use the corrected results for the analysis.

5.2 Renormalization scale

The NLO couplings are usually defined at $\mu = 4\pi F$ or at the ρ mass, $\mu = M_\rho$. Still, in the context of the large N_c expansion these are two very different choices, since the former scales with $\sqrt{N_c}$, deviating from the physical cutoff of

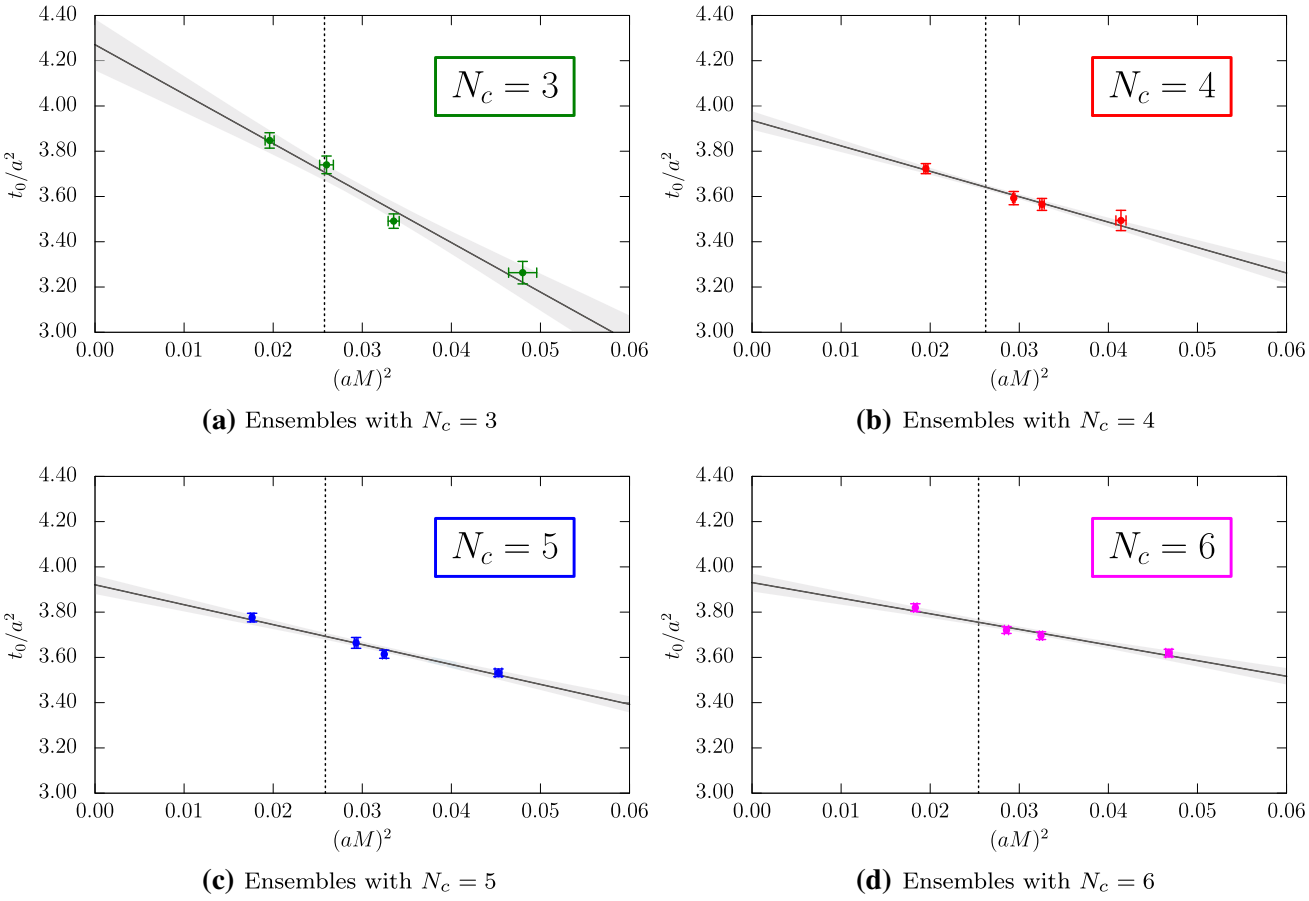

(a) Ensembles with $N_c = 3$ **(b)** Ensembles with $N_c = 4$

(c) Ensembles with $N_c = 5$ **(d)** Ensembles with $N_c = 6$

Fig. 1 Mass dependence of t_0^{imp}/a^2. The vertical line corresponds to the value $M^2 = M_{\text{ref}}^2$

Table 3 Results obtained in the mixed action setup, with Wilson fermions on the sea and twisted mass in the valence sector. We use $c_{sw} = 1.69$, as in the sea sector

Ensemble	am_{cr}	$a\mu_0$	aM_π^{v}	$\lvert am_{pcac}^{\text{v}}\rvert$	aF_π
3A10	−0.4214	0.01107	0.2216 (20)	0.0000 (3)	0.04405 (41)
3A20	−0.4196	0.00781	0.1834 (6)	0.0001 (2)	0.04023 (24)
3A30	−0.4187	0.00632	0.1613 (11)	0.0008 (2)	0.03678 (33)
3A40	−0.4163	0.00513	0.1423 (7)	0.0006 (3)	0.03554 (15)
4A10	−0.3875	0.01030	0.2037 (11)	0.0001 (2)	0.05131 (37)
4A20	−0.3865	0.00844	0.1803 (9)	0.0000 (4)	0.05037 (26)
4A30	−0.3865	0.00778	0.1717 (9)	0.0001 (4)	0.04913 (31)
4A40	−0.3851	0.00546	0.1416 (5)	0.0001 (2)	0.04608 (15)
5A10	−0.3611	0.01225	0.2114 (13)	0.0003 (4)	0.06125 (32)
5A20	−0.3611	0.00906	0.1799 (10)	0.0001 (4)	0.05767 (30)
5A30	−0.3607	0.00824	0.1706 (13)	0.0000 (4)	0.05647 (40)
5A40	−0.3596	0.00509	0.1328 (5)	0.0002 (2)	0.05278 (18)
6A10	−0.3415	0.01298	0.2142 (6)	0.0003 (2)	0.06813 (21)
6A20	−0.3414	0.00956	0.1801 (4)	0.0002 (2)	0.06435 (25)
6A30	−0.3414	0.00803	0.1668 (5)	0.0002 (2)	0.06278 (24)
6A40	−0.3409	0.00542	0.1342 (4)	0.0000 (1)	0.05929 (14)

the chiral effective theory, which is expected to be set by the lighter resonances, such as the ρ. The scale $\mu = 4\pi F$ is instead the scale at which ChPT breaks down, which for large enough N_c is much higher than the scale at which new resonances appear. In the context of large N_c, it is therefore sensible to choose a renormalization scale more closely related to the physical cutoff that does not scale with N_c. Keeping the scale related to $4\pi F$, however, has some advantages for fitting, so we choose:

$$\mu^2 = \frac{3}{N_c}(4\pi F)^2, \tag{32}$$

which has no leading dependence on N_c. Using this scale, the NLO predictions can be conveniently written as:

$$F_\pi = F\left[1 - 2\xi \log\left(\frac{N_c}{3}\xi\right) + 64\pi^2 \xi L_F(\mu)\right], \tag{33}$$

$$\frac{M_\pi^2}{m} = 2B\left[1 + \frac{1}{4}\xi \log\left(\frac{N_c}{3}\xi\right) + 128\pi^2 \xi L_M(\mu)\right], \tag{34}$$

where $m = \mu_0$, the bare twisted mass. Note that in this expression B is bare, since the quark mass is also bare. The value of the non-singlet pseudoscalar normalization constant, Z_P, is thus needed.

5.3 Fitting strategy

Some care is needed to perform the fits in Eqs. (33) and (34). The complication comes from the fact that both coordinates, $(x, y) = (\xi, F_\pi)$ or $(x, y) = (\xi, M_\pi^2/\mu_0)$ have correlated errors. In particular the Ordinary Least Square (OLS) method is not appropriate, since it assumes no errors in x coordinate. An alternative approach is the York Regression (YR) [80], in which the χ^2 function is:

$$\chi^2 = \sum_i \min_{\delta_i}\left[\mathbf{R}_i^T V^{-1} \mathbf{R}_i\right], \tag{35}$$

where we have defined the two-dimensional vectors:

$$\mathbf{R}_i(\delta_i) \equiv (f(x_i + \delta_i) - y_i, \delta_i), \tag{36}$$

where f is the fitting function, and V is the x, y-covariance matrix, estimated using bootstrap samples. In order to account for autocorrelations, we vary the block-size of the bootstrap samples. We find that blocks of ~ 20 units of Montecarlo are sufficient, and we do not observe a clear N_c dependence. We also estimate all the errors of the fit parameters via bootstrap resampling.

5.4 Fit results at fixed N_c

First we consider each N_c separately and perform a fit of the data points to extract F, $L_F(\mu)$ and B, $L_M(\mu)$. The NLO fit results for these quantities are shown respectively in Tables 4 and 5. The N_c dependence of the LECs is shown in Figs. 2 and 3. It can be seen that the scaling is well described by leading and subleading N_c corrections for $N_c = 4$–6, while there seems to be significant $1/N_c^2$ corrections for $N_c = 3$ in the case of F and L_F. In the case of B and L_M errors are larger and there is no sign of $1/N_c^2$. Interestingly, the data suggest that the large N_c limit of $L_M \sim 0$.

Table 4 NLO Fits for F_π for separate values of N_c

N_c	$aF/\sqrt{N_c}$	L_F/N_c	χ^2/dof
3	0.0088 (9)	0.0046 (14)	0.7/2
4	0.0155 (6)	0.0013 (3)	3.9/2
5	0.0175 (4)	0.0011 (2)	2.2/2
6	0.0188 (2)	0.0011 (1)	0.4/2

Table 5 Fits for M_π for separate values of N_c

N_c	aB	L_M/N_c	χ^2/dof
3	1.564 (55)	0.00086 (10)	10.2/2
4	1.560 (37)	0.00064 (7)	1.4/2
5	1.648 (30)	0.00031 (6)	0.1/2
6	1.610 (20)	0.00031 (4)	9.5/2

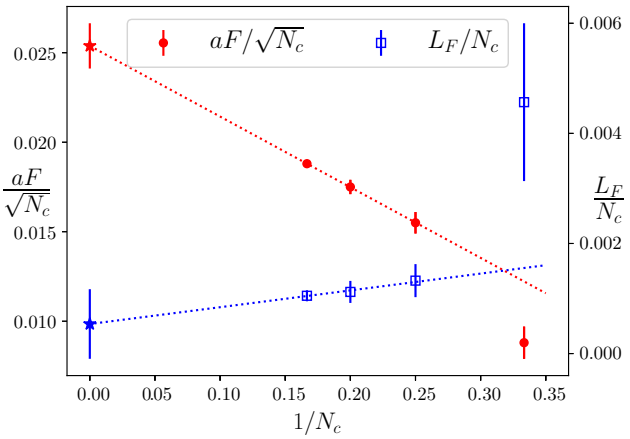

Fig. 2 N_c dependence of $F/\sqrt{N_c}$ (red) and L_F (blue). The dotted lines are the best fits to Eqs. (5) and (7) excluding the data points at $N_c = 3$

5.5 Simultaneous chiral and N_c fits

We now consider a global fit including several data points at different values of N_c. We first perform a $SU(N_f)$-NLO fit to the subset $N_c = 4$–6, including leading and subleading N_c corrections for all the LO and NLO LECs, as parametrized in Eqs. (5) and (7). We linearize the fit by considering the following parametrization

$$F_\pi = \sqrt{N_c}\left(F_0 + \frac{F_1}{N_c}\right)\left[1 - 2\xi \log\left(\frac{N_c}{3}\xi\right)\right] + 64\pi^2 \xi \sqrt{N_c}\left(N_c (FL_F)^{(0)} + (FL_F)^{(1)}\right), \tag{37}$$

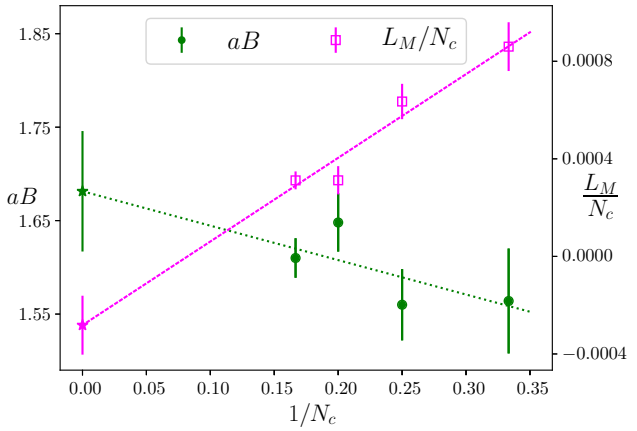

Fig. 3 N_c dependence of B and L_M. The dotted lines are the best fits to Eqs. (5) and (7) including all points

$$\frac{M_\pi^2}{m} = 2\left(B_0 + \frac{B_1}{N_c}\right)\left[1 + \frac{1}{4}\xi \log\left(\frac{N_c}{3}\xi\right)\right] + 256\pi^2\xi\left(N_c(BL_M)^{(0)} + (BL_M)^{(1)}\right), \tag{38}$$

where $(FL_F)^{(0)} \equiv F_0 L_F^{(0)}$, while $(FL_F)^{(1)} \equiv F_1 L_F^{(0)} + L_F^{(1)} F_0$, and $(BL_M)^{(0)} \equiv B_0 L_M^{(0)}$ and $(BL_M)^{(1)} \equiv B_1 L_M^{(0)} + B_0 L_M^{(1)}$.

Secondly, we consider the $U(N_f)$-NNLO expansion, since we have checked that the $U(N_f)$-NLO expressions fit the data very poorly. We also linearize the fit by considering the following fitting functions:

$$F_\pi = \sqrt{N_c}\left(F_0 + \frac{F_1}{N_c} + \frac{F_2}{N_c^2}\right)\left[1 - 2\xi \log\left(\frac{N_c}{3}\xi\right)\right] + 64\pi^2\xi\sqrt{N_c}\left(N_c(FL_F)^{(0)} + (FL_F)^{(1)}\right) + N_c^2\sqrt{N_c}\left(16\pi^2\xi\right)^2 K_F^{(0)}, \tag{39}$$

$$\frac{M_\pi^2}{m} = 2\left(B_0 + \frac{B_1}{N_c} + \frac{B_2}{N_c^2}\right)\left[1 + \frac{1}{4}\xi \log\left(\frac{N_c}{3}\xi\right) + -\frac{1}{4}\left(\xi + \frac{a_0}{N_c^2}\right)\log\left(\frac{N_c}{3}\left(\xi + \frac{a_0}{N_c^2}\right)\right)\right] + 256\pi^2\xi\left(N_c(BL_M)^0 + (BL_M)^{(1)}\right) - 64N_c^2\left(16\pi^2\xi\right)^2 K_M^{(0)}, \tag{40}$$

where

$$a_0 \equiv N_c^2 \frac{M_0^2}{(4\pi F)^2}, \tag{41}$$

and M_0^2 is given by the Witten–Veneziano formula for the η' mass valid in the large N_c limit (see Eq. 13). We use the result for the topological susceptibility from Ref. [59],

$$t_0^2\chi_t = 7.03(13)\cdot 10^{-4}. \tag{42}$$

We convert to lattice units using the value of t_0/a^2 in the previous section and substitute $F \to \sqrt{N_c}F_0$, as extracted from the global F_π fit. We find $a_0 \sim 6.5$, a value we fix in the fit.

In summary we compare the following fits:

(i) Fit 1: $SU(N_f)$-NLO fit to Eqs. (37) and (38) including the data subset N_c = 4-6.
(ii) Fit 2: $U(N_f)$-NNLO expansion fit to Eqs. (39) and (40) including the full data set.

The results for the fitted parameters in the global fits are shown in Tables 6 and 7, and the quality of the fits is shown in Fig. 4a, b. We also quote in Table 8 the results for the NLO LECs from these fits. Errors are large, but there are significant correlations between the parameters as can be seen in Fig. 5.

5.6 Selected results

We will now quote some results that can be inferred from our fits. We first focus on the decay constant in the chiral limit. Using $a = 0.0754(23)$ fm, we get from our fits at fixed $N_f = 4$:

$$\text{Fit1}: \frac{F}{\sqrt{N_c}} = \left(67(3) - 26(4)\frac{N_f}{N_c}\right)(3\%)^a\text{MeV},$$
$$\text{Fit2}: \frac{F}{\sqrt{N_c}} = \left(70(2) - 22(5)\frac{N_f}{N_c} - \frac{86(37)}{N_c^2}\right)(3\%)^a\text{MeV}, \tag{43}$$

where the N_f dependence assumed is the expected one as discussed in sec. 2. Note that no N_f dependence is assumed in the $1/N_c^2$ terms. The first error is just the one obtained from the fits in Table 6 and the second error of 3% is the one corresponding to the lattice spacing determination. For two- and three-flavour QCD we get:

$$\text{Fit1}: \quad F^{N_c=3,N_f=2} = 86(3)\text{ MeV}, \quad F^{N_c=3,N_f=3} = 71(3)\text{ MeV}, \tag{44}$$
$$\text{Fit2}: \quad F^{N_c=3,N_f=2} = 81(7)\text{ MeV}, \quad F^{N_c=3,N_f=3} = 68(7)\text{ MeV}, \tag{45}$$

where we have taken into account the correlations between the different terms in Eq. (43), and we have assumed no N_f dependence on the last term of the Fit 2. These results are in perfect agreement with phenomenological determinations:

$$F^{N_f=2} = 86.2(5)\text{ MeV in Ref. [81]}, \quad F^{N_f=3} \simeq 71.1\text{ MeV in Ref. [82]}, \tag{46}$$

and also lattice results (see Ref. [45]). In addition, we can compare to previous results in the large N_c limit in the quenched approximation:

Table 6 Different fits for the decay constant as described in the text

Fit	F_0	F_1	F_2	$(FL_F)^{(0)}$	$(FL_F)^{(1)}$	$K_F^{(0)}$	χ^2/dof
1	0.0255 (12)	−0.040 (6)	–	$4.7\ (9.5)\cdot 10^{-6}$	$4.8\ (5.1)\cdot 10^{-5}$	–	0.79
2	0.0266 (9)	−0.034 (8)	−0.033 (14)	$-8\ (10)\cdot 10^{-6}$	$5.6\ (4.4)\cdot 10^{-5}$	$7.6\ (6.4)\cdot 10^{-7}$	0.9

Table 7 Different fits for the meson mass as described in the text

Fit	B_0	B_1	B_2	$(BL_M)^{(0)}$	$(BL_M)^{(1)}$	$K_M^{(0)}$	χ^2/dof
1	1.70 (11)	−0.5 (5)	–	−0.00046 (29)	0.0056 (15)	–	2.0
2	1.72 (7)	−1.8 (5)	1.8 (1.5)	−0.00017 (25)	0.0066 (10)	$1.3(9)\cdot 10^{-6}$	2.4

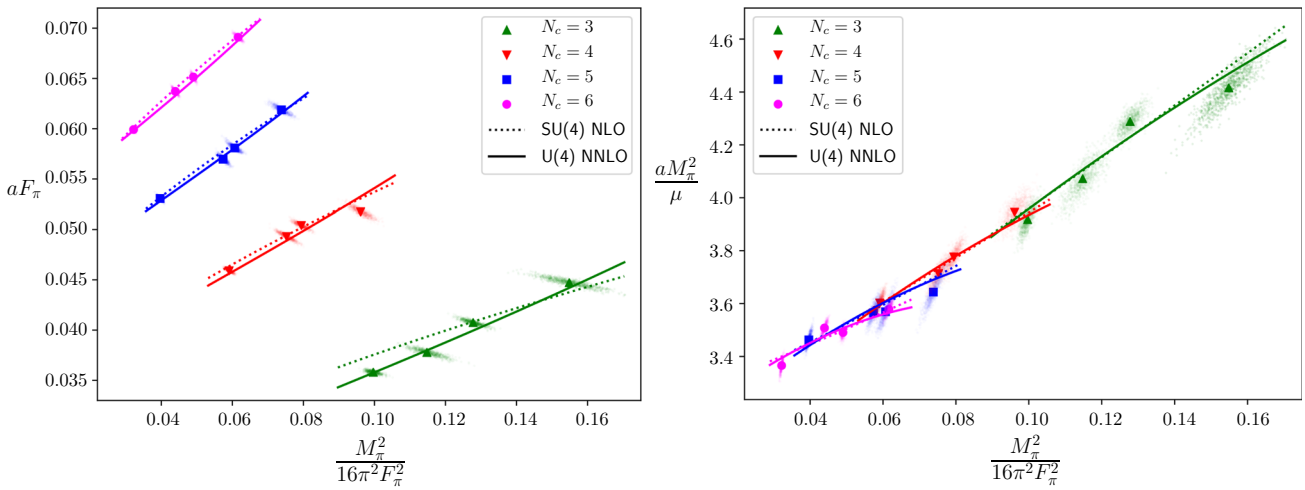

(a) Chiral fits for the decay constant. **(b)** Chiral fits for the meson mass.

Fig. 4 Data and NLO/NNLO fits for the decay constant and meson mass. The central value is shown together with the bootstrap samples used for fitting. The results include finite-volume corrections as in Eq. (30)

$$\left.\frac{F}{\sqrt{N_c}}\right|_{N_c\to\infty} = 56(5)\ \text{MeV},\ \text{Ref. [13]}. \tag{47}$$

This value is 2σ away from the results in Eq. (43). This discrepancy may be explained however with the lack of non-perturbative normalization constant and discretization effects, which in their case are of $O(a)$.

Regarding the coupling, $B \equiv \Sigma/F^2$, we do not have a non-perturbative value of Z_P, up to this factor we get:

$$\begin{aligned}\text{Fit1}: \frac{\Sigma}{F^2} &= Z_P\left(1.70(11) - 0.12(12)\frac{N_f}{N_c}\right),\\ \text{Fit2}: \frac{\Sigma}{F^2} &= Z_P\left(1.72(7) - 0.45(37)\frac{N_f}{N_c} - \frac{1.8(1.5)}{N_c^2}\right).\end{aligned} \tag{48}$$

From Ref. [83], we can obtain the 1-loop perturbative result for the normalization constant:

$$Z_P(N_c = 3) = 0.555, \tag{49}$$

which at the order we are working is independent of N_f. With this, we obtain for $N_c = 3$:

$$\text{Fit 1:}\ N_f = 4 \longrightarrow \frac{\Sigma}{F^2} = 2.26(11)(7)^a\ \text{GeV}, \tag{50}$$

$$N_f = 3 \longrightarrow \frac{\Sigma}{F^2} = 2.31(5)(7)^a\ \text{GeV}, \tag{51}$$

$$N_f = 2 \longrightarrow \frac{\Sigma}{F^2} = 2.35(3)(7)^a\ \text{GeV}, \tag{52}$$

where the first error is systematic, the second comes from the scale setting, and we omit any systematic errors regarding the normalization constant. Combining these results with the ones in Eqs. (44) and (45), we obtain:

$$\Sigma^{1/3}(N_f = 2) = 257(2)(9)^a\ \text{MeV}, \tag{53}$$

$$\Sigma^{1/3}(N_f = 3) = 223(4)(8)^a\ \text{MeV}, \tag{54}$$

which is compatible within 1σ with the numbers quoted in Ref. [45].We can also consider the ratio of condensates for

Table 8 Values for the LECs from the fits in Tables 6 and 7

Fit	$L_F^{(0)}$	$L_F^{(1)}$	$L_M^{(0)}$	$L_M^{(1)}$
1	$1\ (4)\cdot 10^{-4}$	$23\ (13)\cdot 10^{-4}$	$-20\ (15)\cdot 10^{-5}$	$29\ (6)\cdot 10^{-4}$
2	$-3\ (4)\cdot 10^{-4}$	$17\ (18)\cdot 10^{-4}$	$-1\ (1)\cdot 10^{-4}$	$37\ (7)\cdot 10^{-4}$

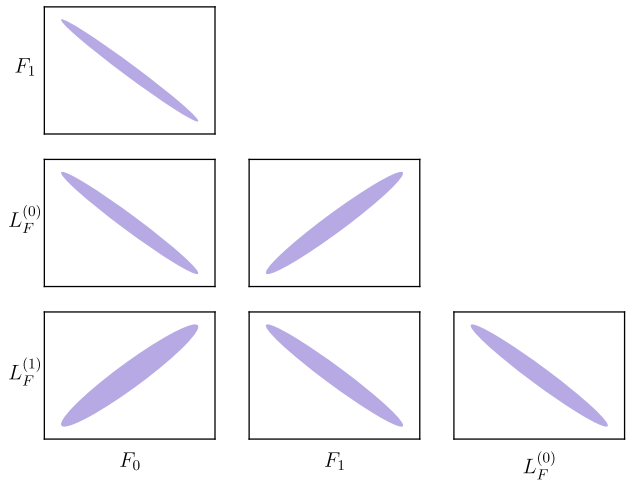

(a) Fit 1 for the decay constant.

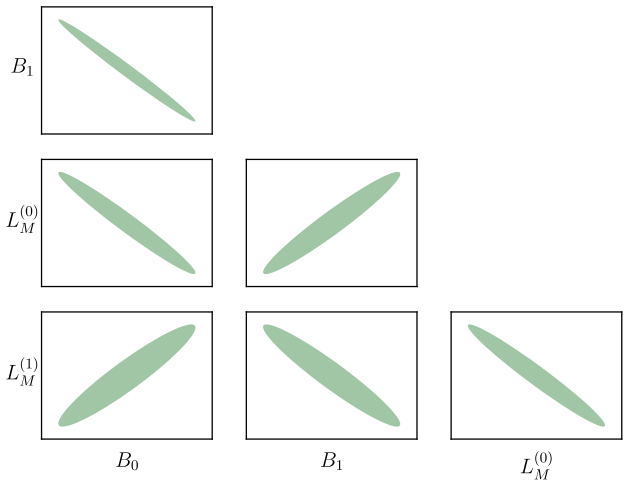

(b) Fit 1 for the mass.

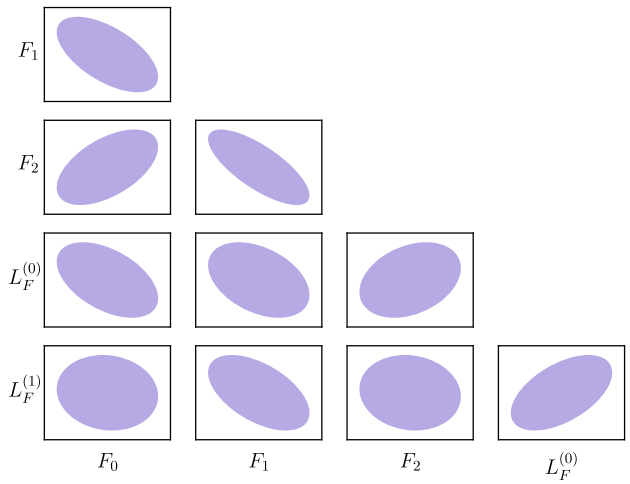

(c) Fit 2 for the decay constant.

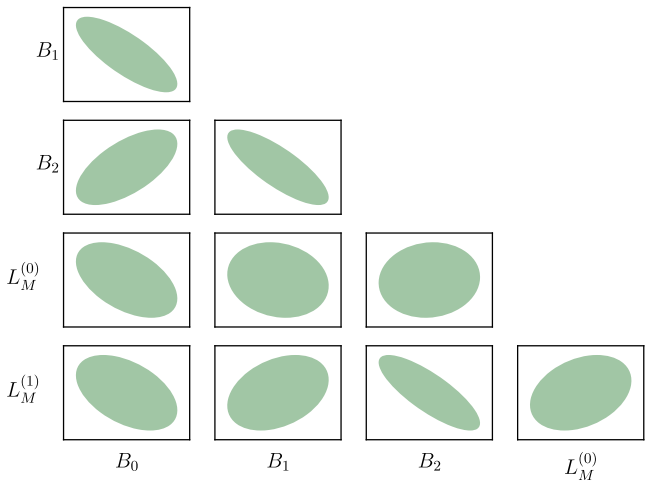

(d) Fit 2 for the mass.

Fig. 5 Correlations between fitted parameters

$N_f = 2$ and $N_f = 3$, where the Z_P factor drops (up to subleading N_f dependence):

$$\frac{\Sigma(N_f=2)}{\Sigma(N_f=3)} = 1.49(10), \tag{55}$$

which shows good agreement with the prediction

$$\frac{\Sigma(N_f=2)}{\Sigma(N_f=3)} = 1.51(11) \text{ in Ref. [47]}. \tag{56}$$

Regarding the NLO LEC for the decay constant, we get from Fit 1:

$$\frac{L_F(\mu)}{N_c}\cdot 10^3 = 0.1(4) + 0.6(3)\frac{N_f}{N_c} + O(N_c^{-2}), \tag{57}$$

while for the NLO LEC for the mass, we can only give the N_c scaling at $N_f = 4$:

$$\frac{L_M^{N_f=4}(\mu)}{N_c}\cdot 10^3 = -0.2(2) + \frac{2.9(6)}{N_c} + O(N_c^{-2}). \tag{58}$$

In the case of Fit 2, we can provide both results together:

$$\begin{aligned}\frac{L_F(\mu)}{N_c}\cdot 10^3 &= -0.3(4)+0.4(4)\frac{N_f}{N_c}+O(N_c^{-2}),\\ \frac{L_M(\mu)}{N_c}\cdot 10^3 &= -0.1(1)+0.9(2)\frac{N_f}{N_c}+O(N_c^{-2}).\end{aligned} \tag{59}$$

From Eqs. 57 and 59, we can infer the $N_c = 3, N_f = 3$ results:

$$\begin{aligned}&\text{Fit1}: L_F(\mu) = 2.1(3)\cdot 10^{-3},\\ &\text{Fit2}: L_F(\mu) = 0.4(2.1)\cdot 10^{-3},\\ &\qquad L_M(\mu) = 2.4(8)\cdot 10^{-3}.\end{aligned} \tag{60}$$

For $N_c = 3$, $N_f = 2$, it is more common to quote $\bar{\ell}_3$ and $\bar{\ell}_4$:

$$\begin{aligned}\bar{\ell}_3 &= 2\log\left(\frac{4\pi F_\pi}{M_\pi^{\text{phys}}}\right) - 16(4\pi)^2 L_M^{N_f=2,N_c=3},\\ \bar{\ell}_4 &= 2\log\left(\frac{4\pi F_\pi}{M_\pi^{\text{phys}}}\right) + 4(4\pi)^2 L_F^{N_f=2,N_c=3}.\end{aligned} \tag{61}$$

This way, we obtain:

$$\begin{aligned}&\text{Fit 1: } \bar{\ell}_4 = 5.1(3),\\ &\text{Fit 2: } \bar{\ell}_3 = 0.4(1.6),\quad \bar{\ell}_4 = 4.1(1.1).\end{aligned} \tag{62}$$

We stress that $U(N_f)$ $\bar{\ell}_3$ in fit 2 is not the same as the standard $\bar{\ell}_3$ in $SU(N_f)$. $\bar{\ell}_4$ agrees instead at 1–2σ with the results quoted in Ref. [45].

5.7 Comments on systematics

The most important systematic uncertainty comes from the finite lattice spacing. Even though a continuum extrapolation would be needed to quantify this error properly, we can get an estimate by comparing the pion mass made of different combination of sea and valence quarks. In particular, Chiral Perturbation Theory in the mixed-action setup predicts that the chiral logs for F_π depend upon the mixed pion mass [84]:

$$M_\pi^{\text{mixed}} \xrightarrow{\text{LO ChPT}} 2B(m^v + m^s), \tag{63}$$

where m^v is the renormalized quark mass in the valence sector and m^s in the sea action. We have measured this mixed pion in one ensemble:

$$\text{Ensemble 3A10} \;\rightarrow\; aM_\pi^{\text{mixed}} = 0.2201(26), \tag{64}$$

obtaining a result which is compatible within errors with both, the sea and valence quark pions.

A different estimate comes from the dependence on c_{sw} in the valence sector. We have recomputed the decay constant for $c_{sw} = 0$ in the 3A10 ensemble, obtaining $[F_\pi]_{c_{sw}=0} = 0.04303(40)$, within 2% of the value at the nominal c_{sw}. The effects of a change in c_{sw} are in principle $O(a^2)$, which can be estimated at $\sim 2\%$ for this observable. This concerns however only the charged meson sector, since the neutral pion is known to have higher discretization effects with twisted mass. That issue is out of the scope of this work, and it will be addressed in future publications. in N_c We end this section with a last word on the chiral fits. We find that our data is well described by ChPT at the order we worked. Still, we cannot exclude that higher order corrections might be relevant in the range of masses we are considering. A robust study on the convergence of ChPT would require simulations at lighter quark masses and a proper continuum extrapolation.

6 Conclusion and outlook

In this work we presented the first lattice determination using dynamical fermions of the N_c scaling of the couplings in the chiral Lagrangian that contribute to the meson masses and decay constants (see Eqs. (43), (48) and Table 8). We have been able to disentangle the leading and subleading terms and we found that the subleading contributions are typically non negligible. In fact, we find that the value for L_M at $N_c = 3$ seems to be dominated by the subleading corrections, and the fit result suggests an accidental cancellation of $2L_8 - L_5$ in the large N_c limit.

From our chiral fits and theoretical expectations, we have been able to infer the values of the couplings for theories with different numbers of flavours, $N_f = 2$ and $N_f = 3$ at $N_c = 3$. We find that our results nicely agree with those in the literature regarding L_F, L_M and F (see for example Ref. [45] for a summary of results). For B we need to improve our determination, including a non-perturbatively determined renormalization factor. On the other hand, as long as this factor has a small N_f dependence, we can estimate the ratio of B and the chiral condensate for $N_f = 2$ and $N_f = 3$. We find excellent agreement with the prediction of paramagnetic suppressions of Refs. [46,47].

We would like to stress that the results presented in this paper are complementary to similar studies that can be performed in reduced models [16–20] or the quenched approximations at large N_c [13], since both of these approaches must yield the leading order result as $N_c \to \infty$. Given the strong correlations presents in our results (see Fig. 5), a precise determination of the dominant N_c term would significantly improve the determination of the subleading N_c corrections, and hence the determination of the physical values at $N_c = 3$. We are willing to provide the bootstrap samples if requested.

As for the future, we would like to mention that our ensembles have a big potential to study other physical observables. We plan to use them to analyse the scaling of other quantities, such as the $K \to \pi$ matrix elements (see [29,62] for

previous results). We also believe that the study of scattering amplitudes is a relevant quantity of study at large N_c: on one hand quantities such as the $I = 2\,\pi\pi$ scattering length give access to LECs of the chiral Lagrangian; on the other hand the study of the behaviour resonances at large N_c is interesting, as it may shed light about their nature [10,11,85,86].

Acknowledgements We thank Andrea Donini for very useful discussions and previous collaboration on related work, as well as M. García Pérez, A. González-Arroyo, G. Herdoíza, A. Ramos, A. Rusetsky, S. Sharpe, C. Urbach and A. Walker-Loud for useful comments and suggestions. We are particularly grateful to Claudio Pica and Martin Hansen for providing us with a $SU(N_c)$ lattice code. This work was partially supported by grant FPA2017-85985-P, MINECO's "Centro de Excelencia Severo Ochoa" Programme under grant SEV-2014-0398, and the European projects H2020-MSCA-ITN-2015/674896-ELUSIVES and H2020-MSCA-RISE-2015/690575-InvisiblesPlus. The work of FRL has also received funding from the European Union Horizon 2020 research and innovation program under the Marie Skłodowska-Curie grant agreement no. 713673 and "La Caixa" Foundation (ID 100010434, LCF/BQ/IN17/11620044). Furthermore, CP thankfully acknowledges support through the Spanish projects FPA2015-68541-P (MINECO/FEDER) and PGC2018-094857-B-I00, the Centro de Excelencia Severo Ochoa Programme SEV-2016-0597, and the EU H2020-MSCA-ITN-2018-813942 (EuroPLEx). We thank Mare Nostrum 4 (BSC), Finis Terrae II (CESGA), Tirant 3 (UV) and Lluis Vives (Servei d'Informàtica UV) for the computing time provided.

Data Availability Statement This manuscript has no associated data or the data will not be deposited. [Authors' comment: We will provide configurations and results from fits upon request.]

References

1. G. 't Hooft, Nucl. Phys. B **72**, 461 (1974)
2. W.A. Bardeen, A.J. Buras, J.M. Gerard, Phys. Lett. B **180**, 133 (1986)
3. W.A. Bardeen, A.J. Buras, J.M. Gerard, Nucl. Phys. B **293**, 787 (1987)
4. R.S. Chivukula, J.M. Flynn, H. Georgi, Phys. Lett. B **171**, 453 (1986)
5. S.R. Sharpe, Phys. Lett. B **194**, 551 (1987)
6. A. Pich, E. de Rafael, Phys. Lett. B **374**, 186 (1996). arXiv:hep-ph/9511465
7. T. Hambye, S. Peris, E. de Rafael, JHEP **05**, 027 (2003). arXiv:hep-ph/0305104
8. A.J. Buras, J.-M. Gérard, W.A. Bardeen, Eur. Phys. J. C **74**(2871), 1401.1385 (2014)
9. H. Gisbert, A. Pich, in *21st High-Energy Physics International Conference in Quantum Chromodynamics (QCD 18) Montpellier, July 2–6, 2018*. arXiv:1810.04904 (2018)
10. J.R. Peláez, J. Nebreda, G. Ríos, Prog. Theor. Phys. Suppl. **186**(113), 1007.3461 (2010)
11. J. Nebreda, J.R. Pelaez, G. Ríos, Phys. Rev. D **84**(074003), 1107.4200 (2011)
12. B. Lucini, M. Teper, JHEP **06**, 050 (2001). arXiv:hep-lat/0103027
13. G.S. Bali, F. Bursa, L. Castagnini, S. Collins, L. Del Debbio, B. Lucini, M. Panero, JHEP **06**, 071 (2013). arXiv:1304.4437
14. T. DeGrand, Y. Liu, Phys. Rev. D **94**, 034506 (2016) [Erratum: Phys. Rev. D **95**(1), 019902 (2017)]. arXiv:1606.01277
15. B. Lucini, M. Panero, Phys. Rep. **526**(93), 1210.4997 (2013)
16. M. García Pérez, A. González-Arroyo, M. Koren, M. Okawa, JHEP **07**(169), 18070.3481 (2018)
17. M. García Pérez, A. González-Arroyo, L. Keegan, M. Okawa, PoS **LATTICE2016**, 337 (2016). arXiv:1612.07380
18. A. González-Arroyo, M. Okawa, Phys. Lett. B **755**, 132 (2016). arXiv:1510.05428
19. A. Hietanen, R. Narayanan, R. Patel, C. Prays, Phys. Lett. B **674**, 80 (2009). arXiv:0901.3752
20. R. Narayanan, H. Neuberger, Phys. Lett. B **616**, 76 (2005). arXiv:hep-lat/0503033
21. T. Appelquist et al. (Lattice Strong Dynamics (LSD)), Phys. Rev. D **89**, 094508 (2014). arXiv:1402.6656
22. T. DeGrand, Y. Liu, E.T. Neil, Y. Shamir, B. Svetitsky, Phys. Rev. D **91**, 114502 (2015). arXiv:1501.05665
23. Y. Aoki et al., (LatKMI), Phys. Rev. D **96**, 014508 (2017). arXiv:1610.07011
24. T. Appelquist et al., Phys. Rev. D **93**, 114514 (2016). arXiv:1601.04027
25. M. Hansen, T. Janowski, C. Pica, A. Toniato, EPJ Web Conf. **175**, 08010 (2018). arXiv:1710.10831
26. D. Nogradi, L. Szikszai (2019), arXiv:1905.01909
27. R.C. Brower, A. Hasenfratz, E.T. Neil, S. Catterall, G. Fleming, J. Giedt, E. Rinaldi, D. Schaich, E. Weinberg, O. Witzel (USQCD) (2019), arXiv:1904.09964
28. L. Del Debbio, PoS **ALPS2018**, 022 (2018)
29. A. Donini, P. Hernández, C. Pena, F. Romero-López, Phys. Rev. D **94**, 114511 (2016). arXiv:1607.03262
30. R.J. Dowdall, C.T.H. Davies, G.P. Lepage, C. McNeile, Phys. Rev. D **88**, 074504 (2013). arXiv:1303.1670
31. R. Frezzotti, V. Lubicz, S. Simula, (ETM), Phys. Rev. D **79**, 074506 (2009). arXiv:0812.4042
32. R. Baron et al., (ETM), JHEP **08**, 097 (2010). arXiv:0911.5061
33. B.B. Brandt, A. Jüttner, H. Wittig, JHEP **11**, 034 (2013). arXiv:1306.2916
34. V. Gülpers, G. von Hippel, H. Wittig, Eur. Phys. J. A **51**, 158 (2015). arXiv:1507.01749
35. A. Bazavov et al., (MILC), PoS **LATTICE2010**, 074 (2010). arXiv:1012.0868
36. S.R. Beane, W. Detmold, P.M. Junnarkar, T.C. Luu, K. Orginos, A. Parreno, M.J. Savage, A. Torok, A. Walker-Loud, Phys. Rev. D **86**, 094509 (2012). arXiv:1108.1380
37. S. Borsanyi, S. Durr, Z. Fodor, S. Krieg, A. Schafer, E.E. Scholz, K.K. Szabo, Phys. Rev. D **88**, 014513 (2013). arXiv:1205.0788
38. S. Dürr et al., (Budapest-Marseille-Wuppertal), Phys. Rev. D **90**, 114504 (2014). arXiv:1310.3626
39. P.A. Boyle et al., Phys. Rev. D **93**, 054502 (2016). arXiv:1511.01950
40. R. Baron et al., (ETM), PoS **LATTICE2010**, 123 (2010). arXiv:1101.0518
41. S. Aoki et al., (PACS-CS), Phys. Rev. D **79**, 034503 (2009). arXiv:0807.1661
42. J. Noaki et al., (JLQCD, TWQCD), Phys. Rev. Lett. **101**, 202004 (2008). arXiv:0806.0894
43. R. Baron et al., JHEP **06**, 111 (2010c). arXiv:1004.5284
44. V. Drach, T. Janowski, C. Pica, EPJ Web Conf. **175**, 08020 (2018). arXiv:1710.07218
45. S. Aoki et al. (Flavour Lattice Averaging Group) (2019), arXiv:1902.08191

46. S. Descotes-Genon, L. Girlanda, J. Stern, JHEP **01**, 041 (2000). arXiv:hep-ph/9910537
47. V. Bernard, S. Descotes-Genon, G. Toucas, JHEP **06**, 051 (2012). arXiv:1203.0508
48. P. Di Vecchia, G. Veneziano, Nucl. Phys. B **171**, 253 (1980)
49. C. Rosenzweig, J. Schechter, C.G. Trahern, Phys. Rev. D **21**, 3388 (1980)
50. E. Witten, Ann. Phys. **128**, 363 (1980)
51. K. Kawarabayashi, N. Ohta, Nucl. Phys. B **175**, 477 (1980)
52. P. Herrera-Siklody, J.I. Latorre, P. Pascual, J. Taron, Nucl. Phys. B **497**, 345 (1997). arXiv:hep-ph/9610549
53. R. Kaiser, H. Leutwyler, Eur. Phys. J. C **17**, 623 (2000). arXiv:hep-ph/0007101
54. J. Bijnens, J. Lu, JHEP **11**, 116 (2009). arXiv:0910.5424
55. J. Bijnens, J. Lu, JHEP **03**, 028 (2011). arXiv:1102.0172
56. J. Bijnens, K. Kampf, S. Lanz, Nucl. Phys. B **873**, 137 (2013). arXiv:1303.3125
57. A.V. Manohar, in *Probing the standard model of particle interactions. Proceedings, Summer School in Theoretical Physics, NATO Advanced Study Institute, 68th session, Les Houches, July 28–September 5, 1997. Pt. 1, 2* (1998), pp. 1091–1169. arXiv:hep-ph/9802419
58. X.-K. Guo, Z.-H. Guo, J.A. Oller, J.J. Sanz-Cillero, JHEP **06**, 175 (2015). arXiv:1503.02248
59. M. Cè, M. García Vera, L. Giusti, S. Schaefer, Phys. Lett. B **762**, 232 (2016). arXiv:1607.05939
60. P. Herrera-Siklody, Phys. Lett. B **442**, 359 (1998). arXiv:hep-ph/9808218
61. L. Del Debbio, A. Patella, C. Pica, Phys. Rev. D **81**, 094503 (2010). arXiv:0805.2058
62. F. Romero-López, A. Donini, P. Hernández, C. Pena, in *36th International Symposium on Lattice Field Theory (Lattice 2018) East Lansing, July 22–28, 2018* (2018). arXiv:1810.06285
63. J. Finkenrath, C. Alexandrou, S. Bacchio, P. Charalambous, P. Dimopoulos, R. Frezzotti, K. Jansen, B. Kostrzewa, G. Rossi, C. Urbach, EPJ Web Conf. **175**, 02003 (2018). arXiv:1712.09579
64. C. Alexandrou et al., Phys. Rev. D **98**, 054518 (2018). arXiv:1807.00495
65. S. Aoki, Y. Kuramashi, Phys. Rev. D **68**, 094019 (2003). arXiv:hep-lat/0306015
66. O. Bar, G. Rupak, N. Shoresh, Phys. Rev. D **67**, 114505 (2003). arXiv:hep-lat/0210050
67. G. Herdoíza, C. Pena, D. Preti, J.A. Romero, J. Ugarrio, EPJ Web Conf. **175**, 13018 (2018). arXiv:1711.06017
68. A. Bussone, S. Chaves, G. Herdoíza, C. Pena, D. Preti, J. A. Romero, J. Ugarrio, in *36th International Symposium on Lattice Field Theory (Lattice 2018) East Lansing, July 22–28, 2018* (2018). arXiv:1812.01474
69. A. Bussone, G. Herdoíza, C. Pena, D. Preti, J.A. Romero, J. Ugarrio (2018), arXiv:1812.05458
70. A. Shindler, Phys. Rep. **461**, 37 (2008). arXiv:0707.4093
71. M. Lüscher, JHEP **08**, 071 (2010) [Erratum: JHEP **03**, 092 (2014)]. arXiv:1006.4518
72. M. Bruno, R. Sommer, (ALPHA), PoS **LATTICE2013**, 321 (2014). arXiv:1311.5585
73. R. Sommer, PoS **LATTICE2013**, 015 (2014). arXiv:1401.3270
74. M. Bruno, T. Korzec, S. Schaefer, Phys. Rev. D **95**, 074504 (2017). arXiv:1608.08900
75. Z. Fodor, K. Holland, J. Kuti, S. Mondal, D. Nogradi, C.H. Wong, JHEP **09**, 018 (2014). arXiv:1406.0827
76. Z. Fodor, K. Holland, J. Kuti, D. Nogradi, C.H. Wong, JHEP **11**, 007 (2012). arXiv:1208.1051
77. O. Bar, M. Golterman, Phys. Rev. D **89**, 034505 (2014) [Erratum: Phys. Rev. D **89**(9), 099905 (2014)]. arXiv:1312.4999
78. J. Gasser, H. Leutwyler, Phys. Lett. B **184**, 83 (1987)
79. G. Colangelo, S. Durr, C. Haefeli, Nucl. Phys. B **721**, 136 (2005). arXiv:hep-lat/0503014
80. D. York, N.M. Evensen, M.L. Martínez, J. De Basabe Delgado, Am. J. Phys. **72**, 367 (2004). https://doi.org/10.1119/1.1632486
81. G. Colangelo, S. Durr, Eur. Phys. J. C **33**, 543 (2004). arXiv:hep-lat/0311023
82. B. Ananthanarayan, J. Bijnens, S. Ghosh, Eur. Phys. J. C **77**, 497 (2017). arXiv:1703.00141
83. C. Alexandrou, M. Constantinou, T. Korzec, H. Panagopoulos, F. Stylianou, Phys. Rev. D **86**, 014505 (2012). arXiv:1201.5025
84. J.-W. Chen, D. O'Connell, A. Walker-Loud, Phys. Rev. D **75**, 054501 (2007). arXiv:hep-lat/0611003
85. V. Bernard, M. Lage, U.G. Meißner, A. Rusetsky, JHEP **01**, 019 (2011). arXiv:1010.6018
86. J. Ruiz de Elvira, U.G. Meißner, A. Rusetsky, G. Schierholz, Eur. Phys. J. C **77**, 659 (2017). arXiv:1706.09015